Journal of Organometallic Chemistry, 427 (1992) 111–123
Elsevier Sequoia S.A., Lausanne
JOM 22373

Synthesis and structure of binuclear thioazobenzene pallada-cycles and their reaction with *m*-chloroperbenzoic acid: formation and structure of dinuclear azophenolates

Surajit Chattopadhyay, Chittaranjan Sinha, Suranjan Bhanja Choudhury and Animesh Chakravorty

Department of Inorganic Chemistry, Indian Association for the Cultivation of Science, Calcutta 700 032 (India)

(Received September 3, 1991)

Abstract

The cyclopalladation of 1,3-bis(2-thioazobenzene)propane (L^1H_2) and its methyl substituted derivative L^2H_2 affords complexes of the type LPd_2Cl_2 (where L represents L^1 or L^2) which have been characterised by spectroscopy and X-ray crystallography. The crystal structure of $L^1Pd_2Cl_2$ has revealed that each azobenzene fragment along with its thioether sulphur acts in the tridentate (C,N,S) fashion and the fourth coordination position is occupied by a chloride ion. The complexes are thus of type $[Pd(C,N,S)Cl]_2$, with a Pd · · · Pd contact of 5.420(1) Å. The metallated carbon atom exerts a strong trans influence on the Pd–S bond. The reaction of LPd_2Cl_2 with *m*-chloroperbenzoic acid leads to smooth oxygen insertion into both the Pd–C bonds to give excellent yields of dinuclear azophenolato complexes *o*-LPd_2Cl_2 having the coordination sphere $[Pd(O,N,S)Cl]_2$. The crystal structure of *o*-$L^1Pd_2Cl_2$ is similar to that of $L^1Pd_2Cl_2$ but with a somewhat longer Pd · · · Pd distance of 5.890(1) Å. The insertion reaction has a negative entropy of activation, in keeping with an associative transition state for the electrophilic incorporation of oxygen. Reduction of the azophenolato complexes with hydrazine hydrate affords the free azophenols (*o*-LH_2) in high yields. Thus organometallic route to *o*-LH_2 from LH_2 is provided.

Introduction

This work stemmed from our interest in the synthesis and reactivity of new cyclopalladated azobenzenes [1–5]. Herein we describe binuclear organometallics of coordination type $[Pd(C,N,S)Cl]_2$ (**1**) derived from thioether substituted bis azobenzenes. The crystal structure of one complex is reported. The reaction of **1**

Correspondence to: Dr. A. Chakravorty, Department of Inorganic Chemistry, Indian Association for the Cultivation of Science, Calcutta 700 032, India.

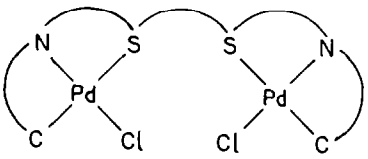

1

with *m*-chloroperbenzoic acid (*m*-CPBA) leads to oxygen insertion into the Pd–C bonds to give the azophenolato complex $[Pd(O,N,S)Cl]_2$. One such complex has been structurally characterised. The treatment of $[Pd(O,N,S)Cl]_2$ with hydrazine hydrate completes a convenient route to the free bis azophenols.

Results and discussion

Synthesis, spectra and structural characterisation

The ligands and complexes described in this paper are shown in Scheme 1, along with the methods used for their synthesis. The azobenzenes, abbreviated as LH_2 (**3**, **4**), are formed by condensation of nitrosoaromatics with the anilines (**2**). These react smoothly with $PdCl_4^{2-}$ to give the orange coloured dinuclear cyclometallates LPd_2Cl_2 (**5**, **6**), which display characteristic absorption bands in the UV-Vis region (Table 1). Their ^1H NMR spectra (Table 2) are well resolved and reveal that the two halves are magnetically equivalent. The N=N and Pd–Cl stretches are observed at ~ 1370 and ~ 320 cm^{-1} respectively; metal coordination expectedly shifts the N=N stretch to lower frequencies relative to that for the free ligand (Table 1).

The presence of the arrangement **1** in the LPd_2Cl_2 complexes has been established in the case of $L^1Pd_2Cl_2$ (**5**) by X-ray crystallography. Molecular views are shown in Fig. 1 and selected bond parameters are listed in Table 3. Each azobenzene fragment along with its thioether sulphur acts in the tridentate (C,N,S) fashion and the fourth coordination position is occupied by a chloride ion. The central methylene carbon of the $-(CH_2)_3-$ bridge is located on a crystallographic two-fold axis.

The three bridge carbon atoms and the two thioether sulphur atoms constitute a planar (mean deviation from best plane 0.027 Å) W-shaped frame to which the coordinated halves are anchored at the sulphur ends (S · · · S length 5.496(1) Å). Each such half incorporating a Pd(C,N,S)Cl fragment constitutes a satisfactory plane with mean deviation of 0.055 Å. The dihedral angle between the planes of two halves is 25.9°, and the Pd · · · Pd contact is 5.420(1) Å. The two halves lie on the same side of the W-frame but are turned away from each other, the Pd–S–S–Pd torsion angle being 88.2°. A view of the molecule projected along the S · · · S axis is shown in Fig. 1(b). A relatively short non-bonded distance is N1 · · · N1a, 3.265(2) Å. In general metal–ligand and other bond distances agree well with those of the two structurally characterised mononuclear Pd(C,N,S)Cl complexes [1,2].

The packing of $L^1Pd_2Cl_2$ molecules in the lattice is noteworthy (Fig. 2). The mean planes of adjacent halves of adjacent molecules are exactly parallel (methylene bridge excluded) and the corresponding interplanar and Pd · · · Pd contacts are 3.423(4) Å and 4.892(1) Å, respectively; the former essentially corresponds to van der Waals distance in crystals of planar aromatic molecules [6,7]. The intermolecular Pd · · · Pd contact is actually shorter than the intramolecular contact.

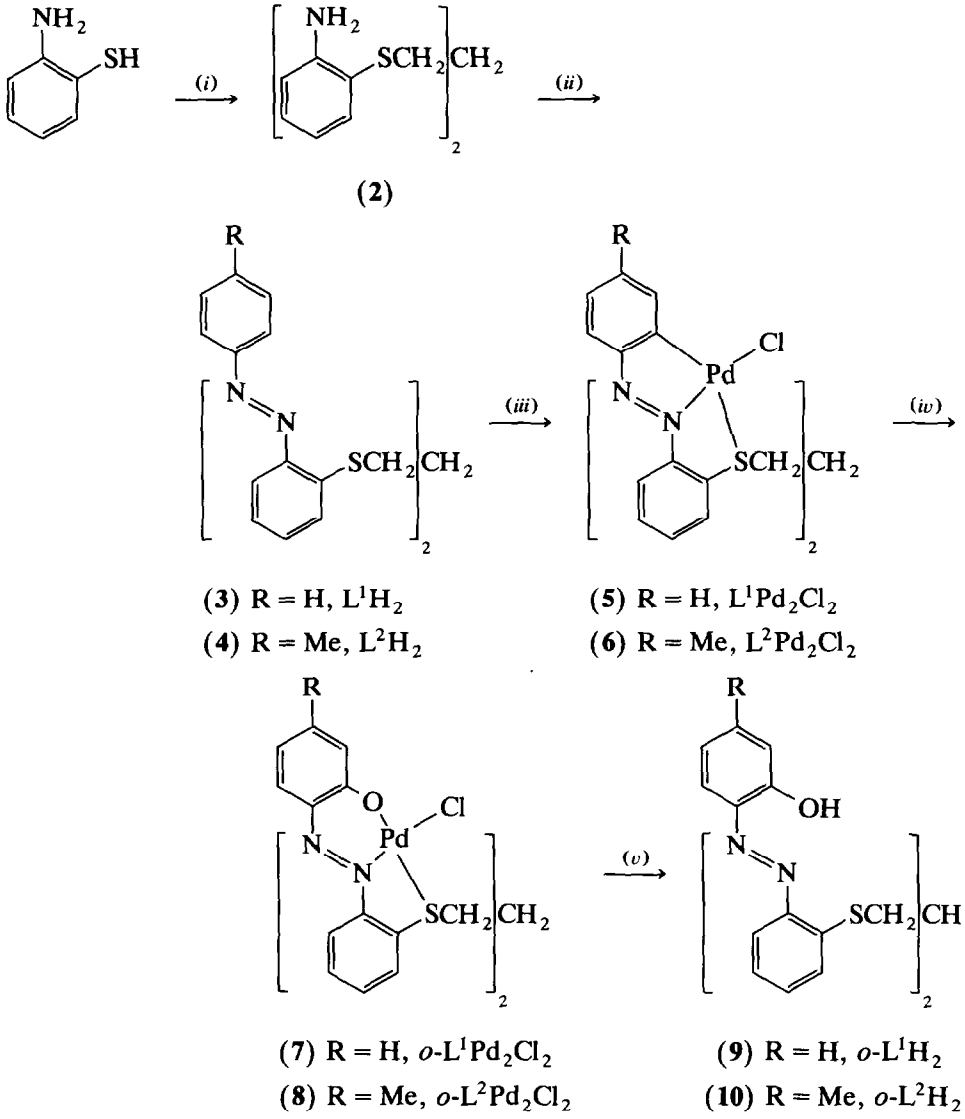

(2)

(3) R = H, L^1H_2
(4) R = Me, L^2H_2
(5) R = H, $L^1Pd_2Cl_2$
(6) R = Me, $L^2Pd_2Cl_2$
(7) R = H, *o*-$L^1Pd_2Cl_2$
(8) R = Me, *o*-$L^2Pd_2Cl_2$
(9) R = H, *o*-L^1H_2
(10) R = Me, *o*-L^2H_2

Scheme 1. (*i*) 1,3-Dibromopropane/Na/EtOH. (*ii*) *p*-RC_6H_4NO/glacial acetic acid. (*iii*) Na_2PdCl_4/EtOH. (*iv*) *m*-CPBA/CH_2Cl_2. (*v*) $N_2H_4 \cdot H_2O$/acetonitrile.

Oxygen insertion into Pd–C bonds: synthesis and characterisation of dinuclear azophenol complexes and liberation of free azophenols from them

Organic peracids are known [3–5,7,8] to undergo insertion of an oxygen atom into the Pd–C bond (eq. 1).

$$Pd\text{–}C + XCO_3H \rightarrow Pd\text{–}OC + XCO_2H \quad (1)$$

The reaction of LPd_2Cl_2 with *m*-CPBA proceeds smoothly in chloroform. The colour of the solution changes progressively from orange-red to violet. From the violet solution, dinuclear azophenol complexes of type *o*-LPd_2Cl_2 were isolated in

Table 1

UV-Vis and IR spectral data

Compound	UV-Vis spectral data [a] λ_{max} (nm) (ϵ(dm^3 mol^{-1} cm^{-1}))	IR spectral data [b]	
		ν(N=N) (cm^{-1})	ν(PdCl) (cm^{-1})
L^1H_2 (3)	390 [c](9000), 315(32000), 260 [c](23300), 230(28400)	1460	
L^2H_2 (4)	385 [c](12400), 325(34700), 265 [c](21500), 230(35400)	1475	
$L^1Pd_2Cl_2$ (5)	515 [c](5000), 480(5800), 405(14300), 375 [c](20600) 355(22900), 320 [c](20200)	1375	320
$L^2Pd_2Cl_2$ (6)	520 [c](7300), 490(8200), 410(15400), 375 [c](18500) 355(19900), 320 [c](17600)	1370	315
o-$L^1Pd_2Cl_2$ (7)	530(14000), 375 [c](13000), 365 [c](18200), 340(22000)	1380	340
o-$L^2Pd_2Cl_2$ (8)	530(13000), 390 [c](15000), 375 [c](19000), 345(20100)	1380	330
o-L^1H_2 (9)	385(9500), 320(16800), 260(14600)	1450	
o-L^2H_2 (10)	390(12700), 320(20500), 270(16000)	1460	

[a] In dichloromethane solution at 298 K. [b] In KBr disk. [c] Shoulder.

excellent yields (7, 8, Scheme 1). Spectral data for o-LPd_2Cl_2 complexes are listed in Tables 1 and 2.

The dinuclear azophenolato formulation is confirmed by an X-ray structural study of o-$L^1Pd_2Cl_2$. Molecular views are shown in Fig. 3. Selected bond distances and angles are listed in Table 3. As in the case of the parent $L^1Pd_2Cl_2$ complex, the o-$L^1Pd_2Cl_2$ molecule is also divided into two equivalent parts by a crystallographic two-fold axis. Here the dihedral angle between the two planar (mean deviation 0.037 Å) halves anchored to the excellently planar (mean deviation 0.006 Å) C_3S_2 W-frame is 36.6° and the Pd ··· Pd contact is 5.890(1) Å. Thus the two halves in o-$L^1Pd_2Cl_2$ are more widely spaced than those in $L^1Pd_2Cl_2$. The Pd–S–S–Pd torsion angle is −99.5°. The N1 ··· N1a distance is 3.320(2) Å.

The Pd–S distance, 2.401(1) Å in $L^1Pd_2Cl_2$, is much longer than that in o-$L^1Pd_2Cl_2$, 2.241(1) Å. In contrast, the Pd–Cl and Pd–N distances in the two molecules are closely similar. The disparity in the Pd–S lengths is attributed to the stronger trans influence of metallated carbon [2,9] in ($L^1Pd_2Cl_2$). The packing of o-$L^1Pd_2Cl_2$ is similar to that of $L^1Pd_2Cl_2$, although along a different crystallographic axis (Fig. 2(b)). In this case the parallel halves of adjacent molecules lie even closer to each other, 3.354(5) Å. The corresponding intermolecular Pd ··· Pd contact is 5.196(1) Å.

The rate of conversion of LPd_2Cl_2 to o-LPd_2Cl_2 by m-CPBA can be conveniently followed spectrophotometrically. The spectral changes are characterised by well-defined isosbestic points as shown in Fig. 4. Rates were determined by monitoring changes in absorption (A_t) at 540 nm with time (t). In the presence of an excess of m-CPBA the plot of $-\ln(A_\infty - A_t)$ against t was excellently linear up to at least 75% of the reaction. The observed rate law is stated in eq. 2.

$$d[o\text{-}LPd_2Cl_2]/dt = k[m\text{-CPBA}]^2[LPd_2Cl_2] \quad (2)$$

The dependency on $[m\text{-CPBA}]^2$ is evident from Fig. 5. Rate constants at various temperatures (291–306 K) and activation parameters are listed in Table 4.

There are no signs that oxygen insertion into the two Pd–C bonds occurs in a stepwise manner. The rate law suggests that both Pd–C bonds are oxidized

Table 2

^{1}H NMR spectral data in $CDCl_3$ [a]

Compound	δ (ppm) (J (Hz))											
	3,3a-H [b]	4,4a-H [c]	5,5a-H [c]	6,6a-H [b]	8,8a-H	9,9a-H	10,10a-H	11,11a-H	12,12a-H	13,13a-H [c]	14,14a-H [d]	Others
L^1H_2 (3)	7.25	7.30	7.35	7.70	7.99	7.53 [e]	7.53 [e]	7.53 [e]	7.99 [b]	3.24	2.20	
	(7.0)	(8.0)	(8.0)	(7.5)	(7.4)				(7.4)	(7.0)	(7.0)	
L^2H_2 (4)	7.26	7.32	7.32	7.72	7.76	7.26 [b]		7.26 [b]	7.76 [b]	3.20	2.20	2.42 [f]
	(8.0)	(8.0)	(8.0)	(8.0)	(7.5)	(8.0)		(8.0)	(7.5)	(7.0)	(7.0)	
$L^1Pd_2Cl_2$ (5)	7.77	7.45	7.56	7.99		7.73 [b]	7.34 [c]	7.34 [c]	7.94 [b]	3.55	2.57	
	(6.8)	(6.8)	(6.8)	(9.0)		(6.8)	(7.4)	(7.4)	(9.0)	(9.0)	(6.0	
$L^2Pd_2Cl_2$ (6)	7.75	7.46	7.49	7.98		7.56 [g]		7.08 [c]	7.82 [b]	3.53	2.54	2.44 [f]
	(6.8)	(7.0)	(7.0)	(6.8)				(7.4)	(9.0)	(9.0)	(6.0)	
o-$L^1Pd_2Cl_2$ (7)	7.73	7.42	7.55	8.09		7.27 [b]	6.88 [c]	7.34 [c]	7.77 [b]	3.55	2.52	
	(6.8)	(9.0)	(9.0)	(6.8)		(9.0)	(9.0)	(9.0)	(6.8)	(6.8)	(6.0)	
o-$L^2Pd_2Cl_2$ (8)	7.65	7.35	7.55	8.08		7.08 [g]		6.70 [b]	7.73 [b]	3.54	2.47	2.38 [f]
	(9.0)	(6.8)	(6.8)	(9.0)				(9.0)	(9.0)	(9.0)	(6.0)	
o-L^1H_2 (9)	7.52	7.36 [e]	7.36 [e]	7.96		7.22 [b]	7.06 [c]	7.36 [c]	7.36 [b]	3.02	2.04	12.80 [h]
	(8.0)			(8.0)		(8.0)	(8.0)	(8.0)	(8.0)	(8.0)	(8.0)	
o-L^2H_2 (10)	7.50	7.32 [e]	7.32 [e]	7.86		6.72 [g]		7.10 [b]	7.52 [b]	3.28	2.14	2.35 [f]
	(8.0)			(8.0)				(8.0)	(7.8)	(8.0)	(8.0)	12.73 [g]

[a] Atom numbering scheme is as in Figs. 1 and 3. [b] Doublet. [c] Triplet. [d] Quintet. [e] Centre of complex multiplet. [f] 10,10a-Me. [g] Singlet. [h] 8,8a-OH.

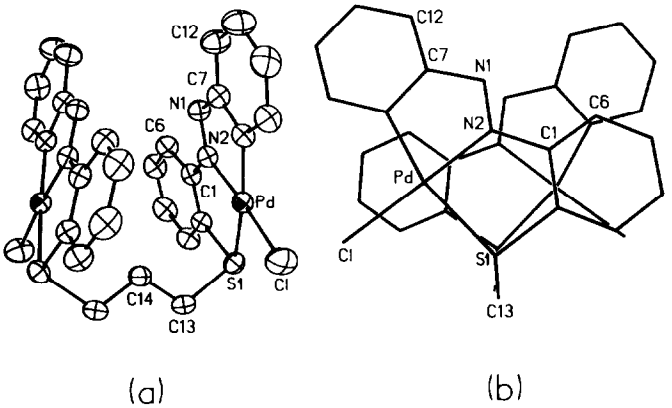

Fig. 1. (a) ORTEP diagram and atom labelling of $L^1Pd_2Cl_2$. All atoms are represented by their 40% probability ellipsoids. (b) Molecular view of $L^1Pd_2Cl_2$ projected approximately along the S · · · S axis.

Table 3

Selected bond lengths (Å) and angles (°) in $L^1Pd_2Cl_2$ (**5**) and *o*-$L^1Pd_2Cl_2$ (**7**)

$L^1Pd_2Cl_2$		*o*-$L^1Pd_2Cl_2$	
Pd–C(8)	1.969(3)	Pd–O	1.983(3)
Pd–S	2.401(1)	Pd–S	2.241(1)
Pd–Cl	2.296(1)	Pd–Cl	2.314(2)
Pd–N(2)	1.971(3)	Pd–N(2)	1.981(3)
N(1)–N(2)	1.276(3)	N(1)–N(2)	1.274(4)
Pd · · · Pd(1)	5.420(1)	Pd · · · Pd(1)	5.890(1)
S(1) · · · S(1a)	5.496(1)	S(1) · · · S(1a)	5.554(1)
N(1) · · · N(1a)	3.265(2)	N(1) · · · N(1a)	3.320(2)
Cl–Pd–C(8)	97.9(1)	Cl–Pd–O	90.5(1)
S(1)–Pd–Cl	97.0(1)	S(1)–Pd–Cl	88.8(1)
Cl–Pd–N(2)	174.5(1)	Cl–Pd–N(2)	176.3(1)
C(8)–Pd–N(2)	79.6(1)	O–Pd–N(2)	93.0(1)
C(8)–Pd–S(1)	165.1(1)	O–Pd–S(1)	177.0(1)
N(2)–Pd–S(1)	85.6(1)	N(2)–Pd–S(1)	87.7(1)
Pd–S(1)–C(13)	103.2(1)	Pd–S(1)–C(13)	103.9(1)
Pd–S(1)–C(2)	94.8(1)	Pd–S(1)–C(2)	97.7(1)

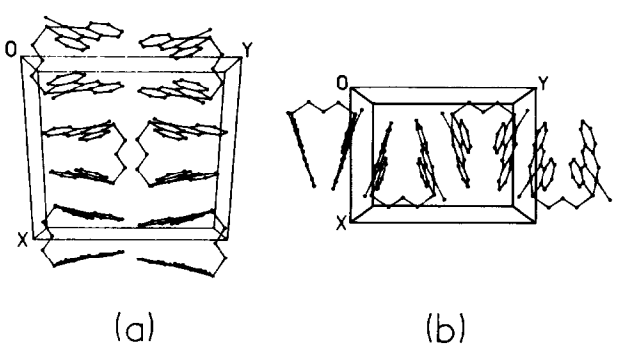

Fig. 2. Packing diagrams of (a) $L^1Pd_2Cl_2$ and (b) *o*-$L^1Pd_2Cl_2$ viewed down the *c*-axis.

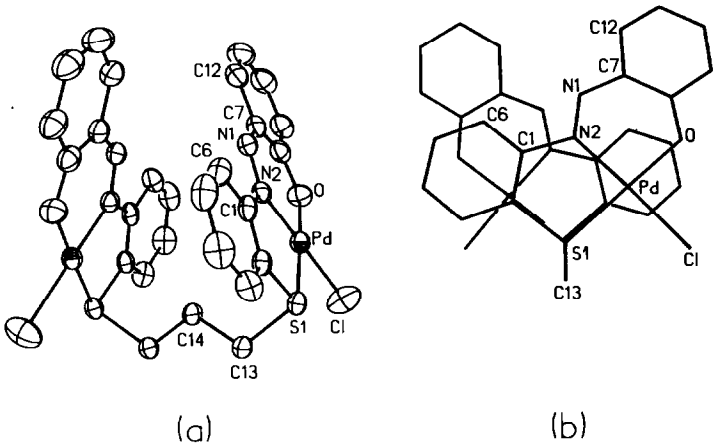

Fig. 3. (a) ORTEP diagram and atom labelling of o-$L^1Pd_2Cl_2$. All atoms are represented by their 40% probability ellipsoids. (b) Molecular view of o-$L^1Pd_2Cl_2$ projected approximately along the S · · · S axis.

virtually simultaneously. We do not have a firm chemical rationale for this. Peracids can exist as dimers [10] and it is possible that the reactive species in the case of LPd_2Cl_2 is actually a dimer.

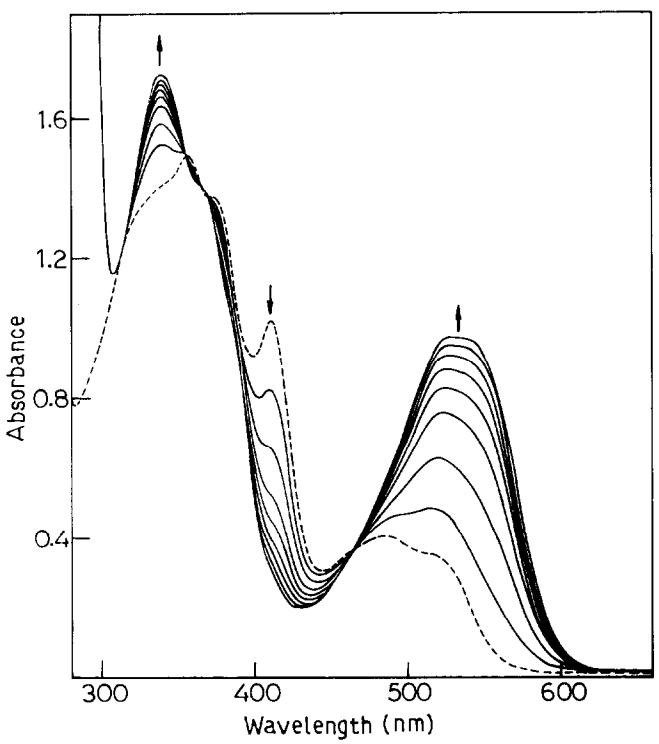

Fig. 4. Spectra of pure $L^1Pd_2Cl_2$ (– – –) and a reaction mixture of $L^1Pd_2Cl_2$ and m-CPBA (———) at 300 K in $CHCl_3$ solution. The arrows indicate increase and decrease of band intensities as the reaction proceeds.

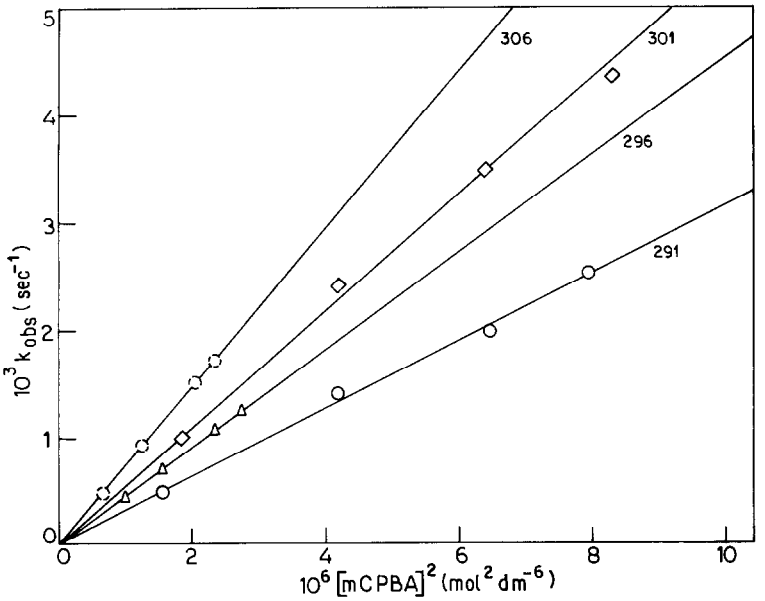

Fig. 5. Variable temperature linear plots of observed rate constants (k_{obs}) *versus* [*m*-CPBA]^2 implying $k_{obs} = k$[*m*-CPBA]^2 (zero intercept).

The mechanism of electrophilic oxygen insertion into the Pd–C bond has been discussed previously [2–5] and is briefly depicted in **11**. The negative entropy of

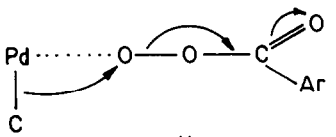

11

activation (Table 4) is in keeping with an associative transition state. The complex $L^2Pd_2Cl_2$ (**6**) carries an electron-releasing methyl group in the metallated ring and oxygen insertion may therefore be expected to be facilitated. This is reflected in the rate data (Table 4).

When *o*-LPd_2Cl_2 is treated with hydrazine hydrate in acetonitrile, metallic palladium is deposited and the colour of the solution changes from violet to yellow and the free azophenol ligand *o*-LH_2 can be isolated from the solution in excellent yield. We thus have a convenient method for synthesis of *o*-LH_2 from LH_2 by an organopalladium route: $LH_2 \rightarrow LPd_2Cl_2 \rightarrow$ *o*-$LPd_2Cl_2 \rightarrow$ *o*-LH_2. Coupling between diazotised amine (**2**) and phenols is unlikely to afford *o*-LH_2 in good yield since the coupling is expected to occur primarily *para* to the phenolic oxygen. The spectral characterisation of *o*-LH_2 ligands is shown in Tables 1 and 2.

Experimental

Disodium tetrachloropalladate(II) was prepared by treating palladium(II) chloride with sodium chloride in water and evaporating the aqueous solution. Commer-

Table 4

Rate constants and activation parameters for oxygen insertion into the Pd–C bonds of $L^1Pd_2Cl_2$ (5) and $L^2Pd_2Cl_2$ (6) by *m*-CPBA

Compound	T (K)	10^3[*m*-CPBA] (mol dm^{-3})	$10^3 k_{obs}$ (s^{-1})	$10^{-3}k$ (mol^{-2} s^{-1})	$\Delta H^{\ddagger}$ (kcal mol^{-1})	$\Delta S^{\ddagger}$ (eu)
$L^1Pd_2Cl_2$ (5)	291	1.241	0.498(6)	0.316(6)	9.1(5)	−16.2(1.6)
		2.040	1.424(6)			
		2.538	2.010(3)			
		2.814	2.559(4)			
	296	0.995	0.451(3)	0.454(7)		
		1.253	0.707(8)			
		1.533	1.071(9)			
		1.655	1.241(4)			
	301	1.356	0.989(4)	0.526(10)		
		2.049	2.421(9)			
		2.530	3.502(8)			
		2.877	4.396(12)			
	306	0.806	0.487(3)	0.741(7)		
		1.109	0.914(8)			
		1.425	1.512(13)			
		1.526	1.730(18)			
$L^2Pd_2Cl_2$ (6)	291	1.114	0.931(3)	0.724(12)	7.3(4)	−20.5(1.4)
		1.789	2.366(9)			
		2.324	3.895(12)			
		2.828	5.761(16)			
	296	1.114	1.240(10)	0.913(28)		
		1.371	2.040(8)			
		1.697	2.917(8)			
		1.979	3.723(7)			
	301	1.140	1.576(3)	1.182(66)		
		1.418	2.381(5)			
		1.817	3.643(9)			
		1.871	4.403(12)			
	306	0.999	1.397(8)	1.392(86)		
		1.285	2.588(6)			
		1.546	3.110(11)			
		1.706	4.261(13)			

cial *m*-chloroperbenzoic acid was purified as previously reported and was used after determination of the active oxygen content by iodometric titration [11,12]. All other chemicals were reagent grade and were used as received. Commercially available BDH silica gel (60–120 mesh) was used for column chromatography.

UV-Vis spectra were recorded on a Hitachi spectrophotometer and IR (4000–200 cm^{-1}) spectra on a Perkin–Elmer 783 spectrophotometer. Proton NMR spectra were recorded for $CDCl_3$ solutions on Varian XL 200 and Bruker 270 MHz FT NMR spectrometers. Elemental analyses were performed with a Perkin–Elmer 240C elemental analyser.

Synthesis

1,3-Bis(2-thioazobenzene)propane, L^1H_2 (3). 1,3-Bis((2-aminophenyl)thio)propane (2) was first prepared as follows. Small pieces of metallic sodium (2.8 g, 0.12

mol) were slowly added to a solution of 2-aminothiophenol (15 g, 0.12 mol) in dry ethanol (66 cm^3). When all the sodium had dissolved, 1,3-dibromopropane (12.5 g, 0.06 mol) was slowly added and the mixture was refluxed for 2 h. The mass was cooled and poured into cold water (150 cm^3). The brown oil that separated was extracted with diethyl ether. The ether was evaporated and the oil was dried over anhydrous Na_2SO_4. Yield 12.5 g (72%). The compound so obtained was used without further purification for the next step.

1,3-Bis((2-aminophenyl)thio)propane (2.9 g, 0.01 mol) and nitrosobenzene (2.2 g, 0.02 mol) were dissolved in glacial acetic acid (30 cm^3). The solution was stirred at 303 K for 2 h. Water (25 cm^3) was then added. The resulting solution was extracted with a petroleum ether/benzene (3:1 v/v) mixture. The mixture was chromatographed on a silica gel column. A deep orange-yellow band was eluted with a petroleum ether/benzene (3:1 v/v) mixture. The solid so obtained by evaporation was purified by repeated crystallisation from petroleum ether/benzene (3:1 v/v) mixture. The yield was 1.15 g (25%), m.p. 41°C. Anal. Found: C, 69.41; H, 5.17; N, 12.07. $C_{27}H_{24}N_4S_2$ calc.: C, 69.23; H, 5.17; N, 11.9%.

The methyl-substituted ligand, L^2H_2 (**4**), was prepared similarly by use of *p*-nitrosotoluene in place of nitrosobenzene. The yield was 30%, m.p. 52°C. Anal. Found: C, 70.90; H, 5.88; N, 11.28. $C_{29}H_{28}N_4S_2$ calc.: C, 70.16; H, 5.65; N, 11.29%.

Dichloro[1,3-bis(2-thioazobenzene)propane-C(8),N(2),S(1),C(8a),N(2a),S(1a)] dipalladium(II), $L^1Pd_2Cl_2$ (5) To an ethanolic solution (10 cm^3) of Na_2PdCl_4 (0.27 g, 0.92 mmol) was added slowly a warm ethanolic solution of L^1H_2 (0.20 g, 0.43 mmol). The colour of the solution gradually changed from yellow to brown-red. The mixture was heated for 1.5 h on a steam bath and the hot solution then left in air to evaporate. The deposited solid was filtered off, washed with ethanol/water (1:3 v/v), then dissolved in dichloromethane (5 cm^3) and chromatographed on a silica gel column prepared in benzene. A deep orange-red band was eluted by acetonitrile/benzene (1:4 v/v) and evaporated *in vacuo*. The solid was crystallised from dichloromethane/hexane (1:5 v/v) mixture to give shining orange crystals in 65% yield. Anal. Found: C, 42.98; H, 2.97; N, 7.39. $C_{27}H_{22}N_4S_2Cl_2Pd_2$ calc.: C, 43.22; H, 2.93; N, 7.47%.

The complex $L^2Pd_2Cl_2$ (**6**) was synthesised similarly using ligand L^2H_2 (**4**) in 60% yield. Anal. Found: C, 44.59; H, 3.54; N, 7.04. $C_{29}H_{26}N_4S_2Cl_2Pd_2$ calc.: C, 44.75; H, 3.34; N, 7.20%.

Dichloro[1,3-bis(2-thioazobenzene-8-phenolato)propane-O,N(2),S(1),O(a),N(2a), S(1a)]dipalladium(II), o-$L^1Pd_2Cl_2$ (7) To a dichloromethane solution (10 cm^3) of $L^1Pd_2Cl_2$ (**5**) (0.10 g, 0.13 mmol) was slowly added a solution of *m*-CPBA (0.37 g, 0.68 mmol) in the same solvent. The mixture was stirred for 3 h, during which the colour changed from orange to violet. The solution was then evaporated to dryness *in vacuo*, and the solid thoroughly washed with ethanol/water (1:1 v/v, 5×5 cm^3), then dissolved in dichloromethane (5 cm^3) and chromatographed on silica gel. A violet band was eluted by acetonitrile/benzene (1:2 v/v) and the eluant evaporated off *in vacuo*. The yield was 60%. The solid was crystallised from dichloromethane/hexane (1:6 v/v) to give pink crystals. Anal. Found: C, 42.42; H, 3.09; N, 6.98. $C_{27}H_{22}N_4O_2S_2Cl_2Pd_2$ calc.: C, 41.45; H, 2.81; N, 7.16%.

The complex *o*-$L^2Pd_2Cl_2$ (**8**) was prepared similarly in 65% yield. Anal. Found: C, 43.21; H, 3.11; N, 7.06. $C_{29}H_{26}N_4O_2S_2Cl_2Pd_2$ calc.: C, 42.98; H, 3.21; N, 6.92%.

Demetallation

To an acetonitrile solution (20 cm^3) of *o*-$L^1Pd_2Cl_2$ (**7**) (0.055 g, 0.07 mmol) was added dropwise a solution of hydrazine hydrate (99%, 0.075 g) in acetonitrile (2 cm^3). The mixture was stirred for 0.5 h during which the colour changed from violet to yellow and black metallic palladium separated. The solution was filtered and the filtrate evaporated *in vacuo*. A dichloromethane solution of the gummy mass was chromatographed on a silica gel column prepared in petroleum ether. A yellow band was eluted with benzene, and evaporation of the eluant *in vacuo* gave pure 1,3-bis(8-hydroxy-2-thioazobenzene)-propane, *o*-L^1H_2 (**9**), in 80% yield. Anal. Found: C, 64.69; H, 4.92; N, 11.12. $C_{27}H_{24}N_4S_2O_2$ calc.: C, 64.80; H, 4.80; N, 11.20%.

The hydroxyazo compound *o*-L^2H_2 (**10**) was prepared similarly from *o*-$L^2Pd_2Cl_2$ in 65% yield. Anal. Found: C, 66.02; H, 5.18; N, 10.53. $C_{29}H_{28}N_4S_2O_2$ calc.: C, 65.91; H, 5.30; N, 10.61%.

Kinetic measurements

Thermostated solutions of reactants were mixed and the mixture was diluted to the required volume and transferred to an absorption cell of 1 cm path length. The increase in absorption at 540 nm was digitally recorded as a function of time. The "infinity" value A_∞ was measured when the intensity change levelled off. In all

Table 5

Crystallographic data for $L^1Pd_2Cl_2$ (**5**) and *o*-$L^1Pd_2Cl_2$ (**7**)

	$L^1Pd_2Cl_2$	*o*-$L^1Pd_2Cl_2$
Formula	$C_{27}H_{22}N_4S_2Cl_2Pd_2$	$C_{27}H_{24}N_4O_2S_2Cl_2Pd_2$
Formula weight	750.3	784.3
Crystal size (mm^3)	0.64×0.36×0.30	0.34×0.30×0.50
Crystal system	Monoclinic	Orthorhombic
Space group	*C2/c*	*Pbna*
a (Å)	16.955(6)	10.398(4)
b (Å)	16.529(6)	13.991(5)
c (Å)	10.990(4)	19.251(10)
β (°)	119.15(2)	
V ($Å^3$)	2689.8(16)	2801(2)
Z	4	4
No. centering reflections	25	25
Centering 2θ	$15° \leqslant 2\theta \leqslant 30°$	$15° \leqslant 2\theta \leqslant 30°$
D_c ($g\ cm^{-3}$)	1.853	1.860
$\mu(M_o - K_\alpha)$ (cm^{-1})	16.95	16.37
2θ limits	2–55	2–55
h, *k*, *l* range	19, 21, ±13	13, 18, 24
No. unique reflections	3033	3190
Observed data $I > 3\sigma(I)$	2644	2278
Parameters refined	334	352
R [a]	0.0245	0.0291
R_w [b]	0.044	0.0401
g in weighting scheme [c]	0.0013	0.0007
Largest peak in final Fourier map (e $Å^{-3}$)	0.32	0.52

[a] $R = \Sigma(|F_o| - |F_c|)/\Sigma|F_o|$. [b] $R_w = [\Sigma w(|F_o| - |F_c|)^2/\Sigma w|F_o|^2]^{1/2}$. [c] $1/[\sigma^2(|F_o|) + g|F_o|^2]$.

Table 6

Atomic coordinates ($\times 10^4$) for $L^1Pd_2Cl_2$ (**5**)

	x	*y*	*z*
Pd	3360(1)	3041(1)	2363(1)
Cl	3094(1)	3866(1)	3804(1)
S(1)	3174(1)	4053(1)	678(1)
N(1)	3898(2)	1575(2)	1627(2)
N(2)	3705(2)	2315(2)	1278(2)
C(1)	3773(2)	2601(2)	116(3)
C(2)	3544(2)	3416(2)	−261(3)
C(3)	3576(2)	3736(2)	−1403(3)
C(4)	3873(3)	3241(2)	−2128(3)
C(5)	4108(2)	2452(2)	−1746(3)
C(6)	4065(2)	2118(2)	−610(3)
C(7)	3799(2)	1399(2)	2783(3)
C(8)	3548(2)	2024(2)	3404(3)
C(9)	3422(2)	1811(2)	4532(3)
C(10)	3542(3)	1025(3)	4991(3)
C(11)	3798(3)	421(2)	4401(4)
C(12)	3925(2)	604(2)	3271(3)
C(13)	4167(2)	4692(2)	1618(3)
C(14)	5000	4193(3)	2500

experiments the concentration of *m*-CPBA was kept high so as to give apparent first order rate constants (k_{obs}). The values of k_{obs} were obtained from the slopes of the plots of $-\ln(A_\infty - A_t)$ *versus* t lines. Values of third order rate constants, k,

Table 7

Atomic coordinates ($\times 10^4$) for *o*-$L^1Pd_2Cl_2$ (**7**)

	x	*y*	*z*
Pd	2086(1)	573(1)	615(1)
Cl	3685(1)	−76(1)	1306(1)
S(1)	3460(1)	553(1)	−281(1)
O	917(3)	650(2)	1427(1)
N(1)	−380(3)	1324(2)	112(2)
N(2)	776(3)	1093(2)	−29(2)
C(1)	1128(4)	1207(2)	−750(2)
C(2)	2385(4)	988(3)	−928(2)
C(3)	2804(4)	1078(3)	−1617(2)
C(4)	1952(5)	1404(3)	−2113(2)
C(5)	710(6)	1621(3)	−1933(2)
C(6)	273(4)	1528(3)	−1252(2)
C(7)	−879(4)	1277(3)	767(2)
C(8)	−244(4)	967(3)	1388(2)
C(9)	−963(5)	1009(3)	2018(2)
C(10)	−2208(5)	1323(4)	2030(3)
C(11)	−2833(5)	1615(4)	1417(3)
C(12)	−2188(4)	1593(3)	807(3)
C(13)	4471(4)	1602(2)	−136(2)
C(14)	3660(5)	2500	0

were obtained from the slopes of the plots of k_{obs} *versus* [*m*-CPBA]^2. Activation parameters were obtained from the Eyring equation. Values of k_{obs}, k, $\Delta H^{\ddagger}$, $\Delta S^{\ddagger}$ and their deviations were calculated by the usual least-squares methods [13]. A minimum of 30 A_t–t points were used in each calculation.

X-Ray diffraction studies

Crystals suitable for X-ray work in both cases were grown by slow diffusion of dichloromethane solutions into hexane at 298 K. Data collection was performed on a Nicolet R3m/V automated diffractometer using graphite monochromated Mo-K_α radiation ($\lambda = 0.71073$ Å). Relevant crystal data and data collection parameters are listed in Table 5.

Intensities were corrected for Lorentz and polarisation effects. An empirical absorption correction was made on the basis of ψ-scans [14]. All calculations, data reduction and structure solutions were performed on a MicroVAX II computer with the SHELXTL-PLUS programs [15]. The positions of the metal atom in each case were determined by the heavy atom method. All non-hydrogen atoms were located from subsequent difference Fourier maps and were made anisotropic. The hydrogen atoms were included at their idealised positions with fixed thermal parameters. Atomic coordinates are listed in Tables 6 and 7.

Tables of H-atom coordinates, thermal parameters, a complete list of bond distances and angles, and lists of structure factors are available from the authors.

Acknowledgements

Crystallography was performed at the National Single Crystal Diffractometer Facility, Department of Inorganic Chemistry, Indian Association for the Cultivation of Science. Financial support received from the Department of Science and Technology, New Delhi and the Council of Scientific and Industrial Research, New Delhi, India, is acknowledged.

References

1 S. Chattopadhyay, C. Sinha, P. Basu and A. Chakravorty, J. Organomet. Chem., 414 (1991) 421.
2 S. Chattopadhyay, C. Sinha, P. Basu and A. Chakravorty, Organometallics, 10 (1991) 1135.
3 C. Sinha, D. Bandyopadhyay and A. Chakravorty, Inorg. Chem., 27 (1988) 1173.
4 A.K. Mahapatra, D. Bandyopadhyay, P. Bandyopadhyay and A. Chakravorty, Inorg. Chem., 25 (1986) 2214.
5 C. Sinha, D. Bandyopadhyay and A. Chakravorty, J. Chem. Soc., Chem. Commun., (1988) 468.
6 D.E. Williams, Acta Crystallogr., Sect. A36 (1980) 715.
7 D. Kathleen, H.J. Milledge and K.V.K. Rao, Proc. R. Soc. London, Ser. A, 255 (1960) 82.
8 B.A. Grigor and A.J. Nielson, J. Organomet. Chem., 129 (1977) C17.
9 A.K. Mahapatra, D. Bandyopadhyay, P. Bandyopadhyay and A. Chakravorty, J. Chem. Soc., Chem. Commun., (1984) 999.
10 R.C. Elder, R.D.P. Curea and R.F. Morrison, Inorg. Chem., 15 (1976) 1623.
11 S. Patai (Ed.), The Chemistry of Peroxides, Wiley, New York, 1983, Chap. 5, p. 134.
12 T.G. Traylor, W.A. Lee and D.V. Stynes, J. Am. Chem. Soc., 106 (1984) 755.
13 A.I. Vogel, A Textbook of Practical Organic Chemistry, 2nd edition, Longman, Green, London, 1956, p. 809.
14 W. Youden, J. Anal. Chem., 19 (1947) 946.
15 A.C.T. North, D.C. Philips and F.S. Mathews, Acta Crystallogr., Sect. A, 24 (1968) 351.
16 G.M. Sheldrick, SHELXTL-PLUS 88, Structure Determination Software Programs, Nicolet Instrument Corp., Madison, WI, 1988.